Physics-Informed Neural Network Estimation of Active Material Properties in Time-Dependent Cardiac Biomechanical Models

Matthias Höfler
IDea_Lab,
NAWI Graz, University of Graz, Austria

Francesco Regazzoni
MOX, Dept. of Mathematics
Politecnico di Milano, Italy

Stefano Pagani
MOX, Dept. of Mathematics
Politecnico di Milano, Italy

Elias Karabelas
Dept. of Mathematics and Scientific Computing
NAWI Graz, University of Graz, Austria

Christoph Augustin
Gottfried Schatz Research Center
Medical University of Graz, Austria

Gundolf Haase
Dept. of Mathematics and Scientific Computing
NAWI Graz, University of Graz, Austria

Gernot Plank
Gottfried Schatz Research Center
Medical University of Graz, Austria

Federica Caforio *
Dept. of Mathematics and Scientific Computing
NAWI Graz, University of Graz, Austria

Abstract

Accurate estimation of active stress parameters is essential for understanding cardiac function, but remains clinically challenging when only imaging-derived displacement and strain data are available. We present a Physics-Informed Neural Networks (PINNs)-based framework for inferring active contractility in time-dependent cardiac biomechanical models directly from such data. The approach incorporates adaptive weighting, residual-based attention, Fourier features, and tailored regularisation strategies, enabling robust reconstruction of active stress fields under noisy conditions and at high spatial resolution. A Pareto front analysis is conducted to assess the influence of loss weight selection on parameter estimation. The algorithm is further validated on tissue inhomogeneity detection, with potential clinical impact in conditions such as cardiac fibrosis and myocardial infarction.

1 Introduction

Estimating the active contractility of the myocardium from imaging data is a key challenge in cardiac mechanics. In pathological conditions such as myocardial infarction, fibrotic tissue loses its contractile properties, and identifying these regions non-invasively is clinically crucial for optimal diagnosis and treatment. Existing data-assimilation and optimisation-based approaches [5] are accurate but

*Correspondence: federica.caforio@uni-graz.at

The Third Austrian Symposium on AI, Robotics, and Vision (AIROV26).

computationally intensive and rely on prior assumptions to condense the complex mechanics into a reduced set of parameters. In this work we propose a novel algorithm based on PINNs [7] that estimates spatially-varying active contractility properties in quasi-static and time-dependent settings, extending the work on passive property estimation of [4].

2 Methods

2.1 Governing equations and active stress model

The displacement field $\mathbf{u}(\mathbf{X}, t) \in \mathbb{R}^3$ solves

$$\rho\, \partial_t^2 \mathbf{u} - \nabla \cdot \mathbf{P}(\mathbf{u}) = \mathbf{0} \quad \text{in } \Omega, \tag{1}$$

with Dirichlet and Neumann boundary conditions on Γ_D and Γ_N, respectively. Here $\mathbf{F} = \mathbf{I} + \nabla\mathbf{u}$ is the deformation gradient, $J = \det(\mathbf{F})$ its Jacobian, and $\mathbf{P}$ the first Piola-Kirchhoff stress. The stress decomposes as $\mathbf{P} = \mathbf{P}_{\text{pas}} + \mathbf{P}_{\text{act}}$, where $\mathbf{P}_{\text{pas}}$ follows the transversely isotropic Guccione model [6] and the active stress acts along the myocyte fibre direction $\mathbf{f}_0$ [1]:

$$\mathbf{P}_{\text{act}} = S_a(t)\, \frac{\mathbf{F}\mathbf{f}_0 \otimes \mathbf{f}_0}{\sqrt{\mathbf{F}\mathbf{f}_0 \cdot \mathbf{F}\mathbf{f}_0}}. \tag{2}$$

The scalar active stress $S_a(t)$ obeys the Bestel–Clément–Sorine (BCS) model [3]:

$$\dot{S}_a = -|a(t)|\, S_a + \sigma_0\, |a(t)|_+, \qquad S_a(0) = 0, \tag{3}$$

where $|a(t)|_+ = \max\{a(t), 0\}$ and $a(t)$ encodes the cardiac cycle. The key structural property of (3) is the linear scaling $S_a(t; \sigma_0) = \sigma_0\, S_a^1(t)$. In diseased tissue, the maximum active stiffness $\sigma_0(\mathbf{x}) \geq 0$ vanishes in fully infarcted regions, making its spatial reconstruction the central inverse problem.

2.2 PINN formulation

PINNs [8] embed physical laws directly into the neural network training loss. The displacement $\mathbf{u}$ and, in heterogeneous settings, the active stress $S_a(\mathbf{x})$ are each parametrised by a dedicated network; unknown parameters are recovered by minimising a weighted sum of data-fidelity and physics residual losses via automatic differentiation.

We consider three settings: (i) *quasi-static homogeneous*: S_a spatially constant; (ii) *quasi-static heterogeneous*: $S_a(\mathbf{x})$ spatially varying; (iii) *time-dependent homogeneous*: σ_0 constant, full dynamic problem solved.

Observation model. Training data are FEM-generated displacements and strains corrupted with Gaussian noise $\boldsymbol{\varepsilon} \sim \mathcal{N}(\mathbf{0}, \sigma^2)$, characterised by limiting dispersion $\text{LD} = 3\sigma/\max(\mathbf{u})$.

Loss function. The PINN minimises $\mathcal{J}_{\text{OBS}} + \mathcal{J}_{\text{PDE}} + \mathcal{J}_{\text{BCN}} + \mathcal{R}_1$,where $\mathcal{J}_{\text{OBS}}$, $\mathcal{J}_{\text{PDE}}$, $\mathcal{J}_{\text{BCN}}$ are weighted mean-squared-error terms for displacement data fidelity, PDE residual $\mathcal{L}$ at interior collocation points, and Neumann boundary condition (BCN) residual, respectively, and $\mathcal{R}_1 = \lambda_w \|\mathbf{w}\|^2$. In the heterogeneous case, a second network $\text{NN}_{S_a}(\mathbf{x}; \mathbf{w}_2)$ models the active stress field and is subject to additional boundary-weighted and total-variation regularisation.

Network architecture and training. $\text{NN}_{\mathbf{u}}$ has layer widths $[32, 16, 8]$ and NN_{S_a} has $[12, 8, 4]$, both with $\tanh$ activations. Dirichlet conditions are enforced exactly via a signed-distance boundary layer [10]. For scar detection, Fourier feature embeddings (frequency 1.0, dim. 24) [11] are applied only to NN_{S_a} to resolve high-frequency scar boundaries. Training uses a two-phase Adam + BFGS scheme; seeds for which the training loss fails to converge below a predefined threshold, independent of the ground-truth solution, are discarded.

Residual-Based Attention (RBA). Following [2], the PDE loss weight is updated spatially at every fifth iteration: $\lambda^{k+1}(\mathbf{x}) = \gamma\lambda^k(\mathbf{x}) + \eta^* e^k(\mathbf{x})/\left\|e^k\right\|_\infty + \lambda_0$, where $e^k(\mathbf{x})$ is the pointwise PDE residual. This concentrates training on high-residual regions and outperforms static and gradient-based adaptive weighting.

Pareto front analysis. We evaluate the apparent Pareto front [9] in the $(\mathcal{J}_{\mathrm{OBS}}, \mathcal{J}_{\mathrm{PDE}})$ plane over a grid of normalised weight triplets $(\tilde{\lambda}_{\mathrm{OBS}}, \tilde{\lambda}_{\mathrm{PDE}}, \tilde{\lambda}_{\mathrm{BCN}})$ summing to 1, identifying the region of weight space yielding accurate parameter recovery. This analysis provides a quantitative interpretation of how increasing the relative weight of PDE and boundary-condition terms improves parameter recovery in the presence of noise, highlighting the regularising role of the physics constraints.

3 Results

In this section we describe the numerical experiments used to assess the proposed PINN framework.

Setup. Synthetic training data are generated via FEM on a $10\,\mathrm{mm}$ cube with Guccione material ($\alpha_P = 0.8\,\mathrm{kPa}$, $\kappa = 650\,\mathrm{kPa}$, $b_{\mathrm{f}} = 18.48$, $b_{\mathrm{t}} = 3.58$, $b_{\mathrm{fs}} = 1.627$), with homogeneous Dirichlet on one face and homogeneous Neumann boundary conditions on the others. Displacement data (500 points quasi-static; 10 000 time-dependent) are corrupted at LD $\in \{0,\ 0.05\}$. An ensemble of randomly initialised networks is trained per case; seeds are discarded if the training loss does not converge below a predefined threshold, regardless of the ground-truth solution.

Homogeneous tissue. In the quasi-static scalar case the method achieves $\epsilon_{S_a;\mathrm{rel}} = 1.24 \times 10^{-2}$ (noiseless) and 4.93×10^{-2} at LD $= 0.05$, with all seeds converging. In the time-dependent case the decoupled formulation yields $\epsilon_{\sigma_0;\mathrm{rel}} = 6.10 \times 10^{-2}$ (noiseless) and 6.48×10^{-2} at LD $= 0.05$. The small degradation between the two noise levels confirms robustness at LD $= 0.05$ (consistent with cardiac MRI).

Pareto front analysis. Figure 1 shows the Pareto front at LD $= 0.05$. Accurate recovery (stars, $\epsilon_{S_a;\mathrm{rel}} < 5\%$) requires higher PDE and Neumann Boundary condition (BCN) weights, confirming that physics regularisation is essential under noise.

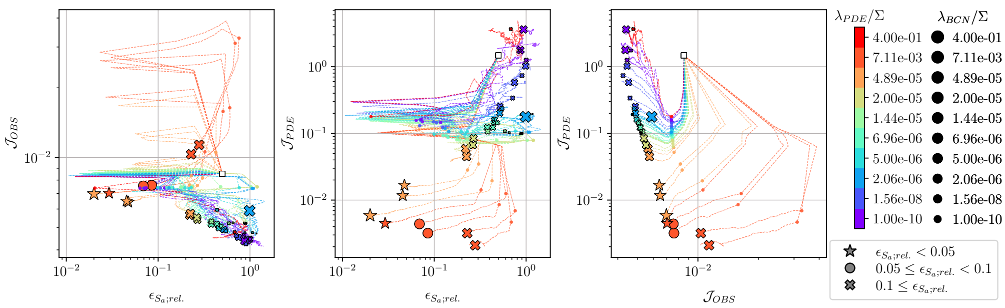

Figure 1: Apparent Pareto front (quasi-static homogeneous, LD $= 0.05$). Colour: $\tilde{\lambda}_{\mathrm{PDE}}$; marker size: $\tilde{\lambda}_{\mathrm{BCN}}$. Stars: $\epsilon_{S_a;\mathrm{rel}} < 5\%$; circles: $< 10\%$; crosses: $\geq 10\%$. Each marker corresponds to a distinct combination of normalised loss weights $(\tilde{\lambda}_{\mathrm{OBS}}, \tilde{\lambda}_{\mathrm{PDE}}, \tilde{\lambda}_{\mathrm{BCN}})$ with $\tilde{\lambda}_{\mathrm{OBS}} + \tilde{\lambda}_{\mathrm{PDE}} + \tilde{\lambda}_{\mathrm{BCN}} = 1$. The coloured trajectories illustrate how the training loss evolves from data-dominated regimes toward physics-dominated ones. Markers on the Pareto frontier represent weight combinations that simultaneously achieve low data-fidelity and low PDE residuals; those achieving $\epsilon_{S_a;\mathrm{rel}} < 5\%$ (stars) cluster in the region with higher $\tilde{\lambda}_{\mathrm{PDE}}$ and $\tilde{\lambda}_{\mathrm{BCN}}$, confirming that physics regularisation is essential under noise.

Scar detection. Figure 2 shows a reconstruction of a spherical cardiac scar with grey zone at LD $= 0.05$. The method accurately detects the scar via post-processing thresholding ($\approx 50\,\mathrm{kPa}$), with minimal misclassification and without prior assumptions on scar shape, number, or topology.

4 Conclusion

We presented a PINN framework for estimating spatially-varying active contractility in nonlinear, time-dependent, anisotropic cardiac tissue. Decoupled space-time formulation, boundary-weighted regularisation, RBA, exact Dirichlet enforcement, and Fourier features enable accurate, noise-robust

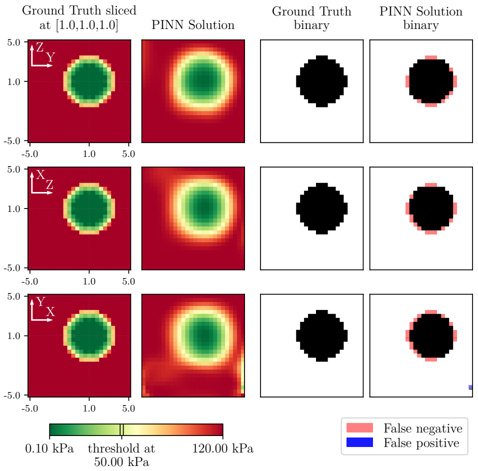

Figure 2: Single spherical scar with grey zone (LD $= 0.05$). Left to right: ground-truth, PINN reconstruction, binary ground-truth (threshold 50 kPa), binary PINN output (red: false negatives; blue: false positives).

reconstruction and scar detection without prior shape knowledge. The Pareto front analysis provides systematic guidance for loss weight selection. To the best of our knowledge, this is the first scientific machine-learning-based method capable of estimating active contractility from displacement and strain data alone from displacement and strain data alone, advancing the state of the art over existing data-assimilation approaches in spatial resolution and freedom from prior shape assumptions [5]. Future work will extend the framework to patient-specific geometries and realistic fibre architectures.

Acknowledgments and Disclosure of Funding

FEM simulations were performed on the Vienna Scientific Cluster (VSC-4, VSC-5) under PRACE projects #71962 and #72420. FC acknowledges support from L'Oréal UNESCO Österreich and the Land Steiermark UFO Grant No. 3026. EK and FC acknowledge the BioTechMed-Graz Young Researcher Grants "CICLOPS" and "CARDIOPHYDAT", respectively. This work was supported in part by the Austrian Science Fund (FWF) under grant 10.55776/P37063 (CMA), by PRIN2022, MUR Italy, P2022N5ZNP, and by the MUR Dipartimento di Eccellenza grant 2023–2027. FC, FR, and SP are members of INdAM-GNCS. **Competing interests:** none.

References

[1] D. Ambrosi and S. Pezzuto. Active stress vs. active strain in mechanobiology: constitutive issues. *Journal of Elasticity*, 107:199–212, 2012. doi: https://doi.org/10.1007/s10659-011-9351-4.

[2] S. J. Anagnostopoulos, J. D. Toscano, N. Stergiopulos, and G. E. Karniadakis. Residual-based attention in physics-informed neural networks. *Computer Methods in Applied Mechanics and Engineering*, 421:116805, Mar. 2024. doi: 10.1016/j.cma.2024.116805.

[3] J. Bestel, F. Clément, and M. Sorine. A biomechanical model of muscle contraction. In *Medical Image Computing and Computer-Assisted Intervention–MICCAI 2001: 4th International Conference Utrecht, The Netherlands, October 14–17, 2001 Proceedings 4*, pages 1159–1161. Springer, 2001. doi: https://doi.org/10.1007/3-540-45468-3.

[4] F. Caforio, F. Regazzoni, S. Pagani, E. Karabelas, C. Augustin, G. Haase, G. Plank, and A. Quarteroni. Physics-informed neural network estimation of material properties in soft tissue nonlinear biomechanical models. *Computational Mechanics*, pages 1–27, 2024. doi: https://doi.org/10.1007/s00466-024-02516-x.

[5] R. Chabiniok, P. Moireau, P.-F. Lesault, A. Rahmouni, J.-F. Deux, and D. Chapelle. Estimation of tissue contractility from cardiac cine-mri using a biomechanical heart model. *Biome-*

chanics and modeling in mechanobiology, 11:609–630, 2012. doi: https://doi.org/10.1007/s10237-011-0337-8.

[6] J. M. Guccione, A. D. McCulloch, and L. K. Waldman. Passive material properties of intact ventricular myocardium determined from a cylindrical model. *Journal of Biomechanical Engineering*, 113(1):42–55, February 1991. doi: 10.1115/1.2894084.

[7] M. HÃ¶fler, F. Regazzoni, S. Pagani, E. Karabelas, C. Augustin, G. Haase, G. Plank, and F. Caforio. Physics-informed neural network estimation of active material properties in time-dependent cardiac biomechanical models. *Journal of the Mechanics and Physics of Solids*, page 106603, 2026. ISSN 0022-5096. doi: https://doi.org/10.1016/j.jmps.2026.106603.

[8] M. Raissi, P. Perdikaris, and G. Karniadakis. Physics-informed neural networks: A deep learning framework for solving forward and inverse problems involving nonlinear partial differential equations. *Journal of Computational Physics*, 378:686–707, February 2019. doi: 10.1016/j.jcp.2018.10.045.

[9] F. M. Rohrhofer, S. Posch, C. Gößnitzer, and B. C. Geiger. Data vs. Physics: The Apparent Pareto Front of Physics-Informed Neural Networks. *IEEE Access*, 11:86252–86261, 2023. doi: 10.1109/ACCESS.2023.3302892.

[10] N. Sukumar and A. Srivastava. Exact imposition of boundary conditions with distance functions in physics-informed deep neural networks. *Computer Methods in Applied Mechanics and Engineering*, 389:114333, Feb. 2022. doi: 10.1016/j.cma.2021.114333.

[11] M. Tancik, P. Srinivasan, B. Mildenhall, S. Fridovich-Keil, N. Raghavan, U. Singhal, R. Ramamoorthi, J. Barron, and R. Ng. Fourier features let networks learn high frequency functions in low dimensional domains. *Advances in neural information processing systems*, 33:7537–7547, 2020.